THE JOURNAL OF BIOLOGICAL CHEMISTRY
Vol. 277, No. 11, Issue of March 15, pp. 8912–8919, 2002
Printed in U.S.A.

Histidines 578 and 587 in the S_5-S_6 Linker of the Human *Ether-a-gogo Related Gene-1* K^+ Channels Confer Sensitivity to Reactive Oxygen Species*

Received for publication, November 28, 2001, and in revised form, December 21, 2001
Published, JBC Papers in Press, December 26, 2001, DOI 10.1074/jbc.M111353200

Anna Pannaccione, Pasqualina Castaldo, Eckhard Ficker‡, Lucio Annunziato, and Maurizio Taglialatela§

From the Unit of Pharmacology, Department of Neuroscience, School of Medicine, University of Naples Federico II, Naples 80131, Italy

The K^+ channels encoded by the human *Ether-a-gogo Related Gene-1* (*hERG1*) are crucially involved in controlling heart and brain excitability and are selectively influenced by reactive oxygen species (ROS). To localize the molecular regions involved in ROS-induced modulation of hERG1, segmental exchanges between the ROS-sensitive hERG1 and the ROS-insensitive bovine ether-a-gogo gene (bEAG) K^+ channels were generated, and the sensitivity of these chimeric channels to ROS was studied with the two-microelectrode voltage-clamp technique upon their expression in *Xenopus* oocytes. Substitution of the S_5-S_6 linker of hERG1 with the corresponding bEAG region removed channel sensitivity to ROS, whereas the reverse chimeric exchange introduced ROS sensitivity into bEAG. Mutation of each of the two hERG1 histidines at positions 578 and 587 within the S_5-S_6 linker generated K^+ channels insensitive to modulation by ROS. In addition, the two iron chelators desferrioxamine (1 mM) and *o*-phenanthroline (0.2 mM) significantly inhibited hERG1 outward K^+ currents and prevented hERG1 inhibition induced by the ROS-scavenging enzyme catalase (1000 units/ml). Finally, the hERG1-inhibitory effect exerted by the iron chelators was prevented by the hERG1 H578D/H587Y double mutation. Collectively, the results obtained suggest that histidines at positions 578 and 587 in the S_5-S_6 linker region of hERG1 K^+ channels are crucial players in ROS-induced modulation of hERG1 K^+ channels.

Oxidation and reduction reactions occurring during aerobic respiration can trigger the formation of reactive oxygen species (ROS),[1] a family of molecules that includes superoxide ($O_2^{\cdot-}$), hydroxyl radical ($^{\cdot}OH$), and hydrogen peroxide (H_2O_2), each having specific half-life, diffusibility, and biological reactivity (1). ROS have been proposed as crucial regulators of cellular responses in several pathophysiological states, such as cardiovascular (2) and neurodegenerative disorders (3), senescence (4), and programmed cell death (5).

Oxidative stress refers to the imbalance between ROS production and cellular antioxidant defense systems (6). Iron ions have a primary role in the induction of oxidative stress, acting as catalysts in the Fenton reaction, which leads to the conversion of the highly diffusible, slow reacting H_2O_2 into the highly reactive and potent oxidant $^{\cdot}OH$ (7). In addition, oxidative stress is also influenced by nitric oxide ($NO^{\cdot}$) and other reactive nitrogen species (RNS) (8), which have been shown to exert both pro- and antioxidant effects during ischemia-reperfusion injury, depending on their cellular sources and on the stage of evolution of the ischemic process (9, 10).

Changes in protein function induced by ROS has been recognized as being crucial for oxidative stress-mediated pathophysiological changes. Maximal sensitivity to ROS is conferred by amino acids containing sulfur atoms (cysteine and methionine), hydroxyl groups (tyrosine), or aromatic rings (histidine, phenylalanine, and tryptophan) (11). Interestingly, histidines in proteins are often associated with transition metals, particularly with redox-active iron ions, and histidines themselves are vulnerable to metal-catalyzed free radical reactions (12). Oxidative modification of histidine residues may lead to their conversion to asparagine, aspartate, or 2-oxo-histidine (13).

K^+ channels play a crucial role in shaping the electrical activity of neuronal and cardiac cells, and modification of K^+ channel activity by ROS and RNS may lead to drastic changes in the excitability of these tissues, such as those occurring during ischemia-reperfusion events (14); furthermore, the heterogeneity of the K^+ channel subsets expressed in specific cells has also been suggested to underlie their different response patterns to hypoxic/anoxic episodes (15). The K^+ channels encoded by the human *Ether-a-gogo Related Gene-1* (*hERG1*) play a crucial role in excitable tissues (16). In fact, in cardiac tissue, *hERG1* encodes for a K^+ current having the biophysical and pharmacological properties of native cardiac I_{Kr}, one of the

* The study was supported in part by the following grants: Telethon 1058; National Research Council (CNR) 97.01233.PF49, 98.03149.CT-04, 99.02614.CT04, 99.00495.PF49, 01.00804.PF49; Italian Ministry of the University and Scientific and Technological Research (MURST) Cofinanziamento (COFIN) 1999 and COFIN 2001 (to M. T.); and by CNR 98.01048.CT04, 98.00062.PF31, 99.02371.CT04, 99.000192.PF31, 01.00169.PF31, 00.D132–001, MURST COFIN 2000; Regione Campania and Istituto Superiore di Sanità (to L. A.). The costs of publication of this article were defrayed in part by the payment of page charges. This article must therefore be hereby marked "*advertisement*" in accordance with 18 U.S.C. Section 1734 solely to indicate this fact.

‡ A Visiting Scientist at the Section of Pharmacology, Dept. of Neurosciences, School of Medicine, University Naples Federico II, Naples, Italy, on leave from the Rammelkamp Center for Education and Research, Case Western Reserve University, School of Medicine, Cleveland, OH 44109-1998.

§ To whom correspondence should be addressed: Section of Pharmacology, Dept. of Neuroscience, School of Medicine, Via. S. Pansini 5, Naples 80131, Italy. Tel.: 39-081-746-3318; Fax: 39-081-746-3323; E-mail: mtaglial@unina.it.

[1] The abbreviations used are: ROS, reactive oxygen species, $NO^{\cdot}$, nitric oxide; RNS, reactive nitrogen species; $O_2^{\cdot-}$ superoxide anion; $^{\cdot}OH$, hydroxyl radical; H_2O_2, hydrogen peroxide; *bEAG*, bovine *ether-a-gogo gene*, *hERG1*, human *Ether-a-gogo Related Gene-1*; *rERG2* and *rERG3*, rat *ether-a-gogo related genes 2* and *3*; MDA, malondialdehyde; NOC, diethylenetetraamine NONOate; Fe/Asc solution, iron- and ascorbate-containing solution; DFX, desferrioxamine; PHE, *ortho*-phenanthroline; $[K^+]_e$, extracellular K^+ concentrations; CAT, catalase.

action potential repolarizing currents (17). Alteration in hERG1 K^+ channels function prompted by drugs and/or gene defects are responsible for the cardiac arrhythmias occurring during the Long QT syndrome (18). In neuronal cells, hERG1 K^+ channels have been implicated in the changes of the resting membrane potential associated with the cell cycle (19), in the control of neuritogenesis and differentiation (20), and in spike-frequency adaptation (21).

Recent studies from our laboratory suggest that hERG1 K^+ channels are influenced by ROS and NO· (22, 23). In particular, the outward currents carried by hERG1 K^+ channels heterologously expressed in *Xenopus* oocytes were enhanced by perfusion with a solution containing iron sulfate and ascorbic acid (Fe/Asc), a widely used experimental condition to promote oxidative stress (1), and were suppressed by the ROS-detoxifying enzyme catalase. In addition, both endogenously produced or pharmacologically delivered NO· was able to inhibit resting hERG1 outward currents and prevented their stimulation by Fe/Asc. These effects appeared to be indirect actions of the gaseous mediator on hERG1 currents, attributable to the potent antioxidant properties of NO· (1, 24). The biophysical mechanism by which ROS and RNS modulated hERG1 outward currents without affecting the inward current component was a depolarizing and hyperpolarizing shift, respectively, of the voltage dependence of the steady-state inactivation curve (22, 23, 25).

Among the K^+ channels investigated, the described modulation by ROS appears to be highly selective for hERG1. In fact, ROS did not affect any channels that were only distantly related to hERG1 (rKv2.1, rKv3.1 and mK_{IR} 2.1) or more closely related to hERG1 (bEAG, rERG2, and rERG3) (16, 26). In the present experiments, to localize the molecular regions involved in ROS-induced modulation of hERG1, we have taken advantage of the similarities between the primary sequence of hERG1 and the ROS-insensitive channel bEAG to generate several chimeras encompassing different regions of the genes encoding for these two K^+ channel subunits. The results obtained suggested that a critical region for ROS-induced modulation was localized in a 30-amino acid stretch located within the S_5-S_6 linker region of hERG1. Within this region, the substitution of each of the two histidines at positions 578 and 587 in hERG1 with the corresponding bEAG amino acid removed channel sensitivity to ROS-induced modulation, thus highlighting their participation in the important regulatory mechanism of hERG1 K^+ channels.

EXPERIMENTAL PROCEDURES

Xenopus Oocytes Isolation—*Xenopus* oocytes dissociation, maintenance, and microinjection followed standard procedures (23). Briefly, ovarian lobes were surgically removed from adult female *Xenopus laevis* frogs (Rettili di Schneider, Varese, Italy) and placed in 100-mm Petri dishes containing a Ca^{2+}-free solution of the following composition (in millimolar): 82.5 NaCl, 2 KCl, 1$MgCl_2$, 5 HEPES, 2.5 pyruvic acid, 100 units/ml penicillin, and 100 μg/ml streptomycin, pH 7.5, with NaOH. After four extensive washes, the oocytes (stages V–VI) were dissociated by collagenase treatment (type IA, 45–80 min at a concentration of 2 mg/ml). Dissociated oocytes were then placed in a Ca^{2+}-containg solution of the following composition (in millimolar): 100 NaCl, 2 KCl, 1.8 $CaCl_2$, 1 $MgCl_2$, 5 HEPES, 2.5 pyruvic acid, 100 units/ml penicillin, and 100 μg/ml streptomycin, pH 7.5, with NaOH, in a 19 °C incubator and used for the experiments on the following day.

Determination of Lipid Peroxidation in Xenopus Oocytes—Lipid peroxidation in *Xenopus* oocytes was determined by assaying the intracellular malondialdehyde (MDA) production by means of the 2-thiobarbituric acid test (22), using previously described procedures (27). MDA, in the cell homogenate, was measured using a PerkinElmer Life Sciences LS5B spectrophotofluorometer (excitation 495 nm, emission 530 nm).

Molecular Biology and Oocyte Injection—The cloning of *hERG1* from human hippocampus (16) (GenBank™ accession number 04270) and of the bovine isoform of *EAG* from brain tissue (28) (*bEAG*, GenBank™ accession number Y13430) has been already described. Both *bEAG* and *hERG1* cDNAs were subcloned into a modified pSP64 vector. The engineering of some of the constructs used in the present study has been already described (29). Briefly, for engineering of the chimeric constructs *hERG1* (*bEAG* S_1/S_6), *hERG1* (*bEAG* S_4-S_5 *linker*/S_6), and *bEAG* (*hERG1* S_4-S_5 *linker*/S_6), the S_1-S_6 core regions of *hERG1* and *bEAG* were subcloned into pBluescript as *Bst*EII-*Xho*I and *Bst*BI-*Kpn*I fragments, respectively. By use of codon redundancy, the following silent restriction sites were introduced into *hERG1 Bst*EII-*Xho*I: *Nar*I (A to G at *hERG1* 1359), *Mlu*I (G to A at *hERG1* 1782), and *Kpn*I (C to G at *hERG1* 2199). In addition, an *Nar*I site was destroyed at *hERG1* 1329 (C to G). The *Mlu*I and *Kpn*I sites in *hERG1* were introduced in positions equivalent to the naturally occurring *Mlu*I and *Kpn*I restriction sites in *bEAG*. In *bEAG Bst*BI-*Kpn*I, a silent *Nar*I site (A to G at *bEAG* 803) was engineered in a position equivalent to the one introduced into hERG1 sequence. For the construction of *hERG1* (*bEAG* S_1-S_6), the *Nar*I-*Kpn*I fragment was excised from the *bEAG Bst*BI-*Kpn*I construct in pBluescript and swapped with the corresponding *hERG1* fragment in *hERG1*-pBluescript. In a final step, the *Bst*EII-*Xho*I fragment was excised and subcloned into full-length *hERG1*-pSP64 from which the wild-type *Bst*EII-*Xho*I fragment had been removed. For construction of *bEAG* (*hERG1* S_4-S_5 *linker*/S_6) and *hERG1* (*bEAG* S_4-S_5 *linker*/S_6), *Mlu*I-*Kpn*I fragments were excised and subcloned into the opposite pBluescript plasmids. In a second step, *Bst*EII-*Xho*I and BstBI-*Kpn*I fragments were excised and subcloned into full-length *hERG1*-pSP64 and *bEAG*-pSP64, respectively.

Chimeric constructs *hERG1* (*bEAG* S_5-S_6 *linker*), *hERG1* (*bEAG* *573*/*602*), and point mutations *hERG1* H578D, *hERG1* H587Y, and *hERG1* H578D/H587Y were generated by overlap extension polymerase chain reaction using the *Bst*EII-*Xho*I *hERG1* cassettes generated in pBluescript in which the *Mlu*I and *Kpn*I had been introduced as previously described. For all these constructs, the entire *Mlu*I-*Kpn*I cassettes were manually sequenced before to subcloning into full-length *hERG1*-pSP64.

cDNAs from all these constructs were linearized with the restriction enzymes *Eco*RI or *Eco*RV, and cRNAs were *in vitro* transcribed from linearized cDNAs by means of commercially available kits (mCAP, Stratagene), using SP6 RNA polymerase. RNAs were stored in a stock solution (250 ng/μl) at −20 °C in 0.1 M KCl. One day after isolation, *Xenopus* oocytes were microinjected with 50 nl of the respective cRNA stock solution or appropriate dilutions.

Electrophysiology—2–10 days after the cRNA microinjection, K^+ currents expressed were measured by the two microelectrode voltage-clamp technique using a commercially available amplifier (Warner OC-725A, Warner Instrument Corp.). Current and voltage electrodes were filled with 3 M KCl, 10 mM HEPES (pH 7.4; ~1 MΩ of resistance). The bath solution contained (in millimolar): 88 NaCl, 10 KCl, 2.6 $MgCl_2$, 0.18 $CaCl_2$, 5 HEPES, pH 7.5 (ND88). This solution was perfused in the recording chamber at a rate of about 0.2 ml/min. Data were stored on the hard disc of a 486 IBM compatible computer for off-line analysis. The pCLAMP (version 6.0.2, Axon Instruments, Burlingame, CA) software was used for data acquisition and analysis. Currents were recorded at room temperature. Oocytes that showed signs of membrane deterioration during the experiment (an increase in the holding current at −90 mV of more than 200 nA) were excluded from the electrophysiological analysis.

Drugs and Statistics—All the materials used were purchased from Sigma Chemical Co. (Milan, Italy); the NO· donor diethylenetetraamine NONOate (NOC) was obtained from Cayman Chemical (Ann Arbor, MI). Iron sulfate and ascorbate stock solutions (10 and 25 mM, respectively) were prepared daily and stored in light-protected tubes to avoid spontaneous oxidation. All solutions were prepared fresh daily, before the execution of the experiments. Statistical significance between the data was obtained by means of the Student *t* test. When appropriate, data are expressed as the mean ± S.E. In the figures *asterisks* denote values statistically different from the controls ($p < 0.05$).

RESULTS

Effect of Fe/Asc Perfusion on the K^+ Channels Encoded by hERG1, bEAG, and hERG1/bEAG Chimeras Expressed in Xenopus Oocytes—hERG1 K^+ channels expressed in *Xenopus* oocytes were activated by depolarizing pulses above −60 mV, displayed pronounced inward rectification at positive potentials (>0 mV) due to a fast C-type inactivation process (17, 25), and were specifically modulated by ROS (22). In fact, perfusion of hERG1-expressing oocytes with the ROS-producing Fe/Asc

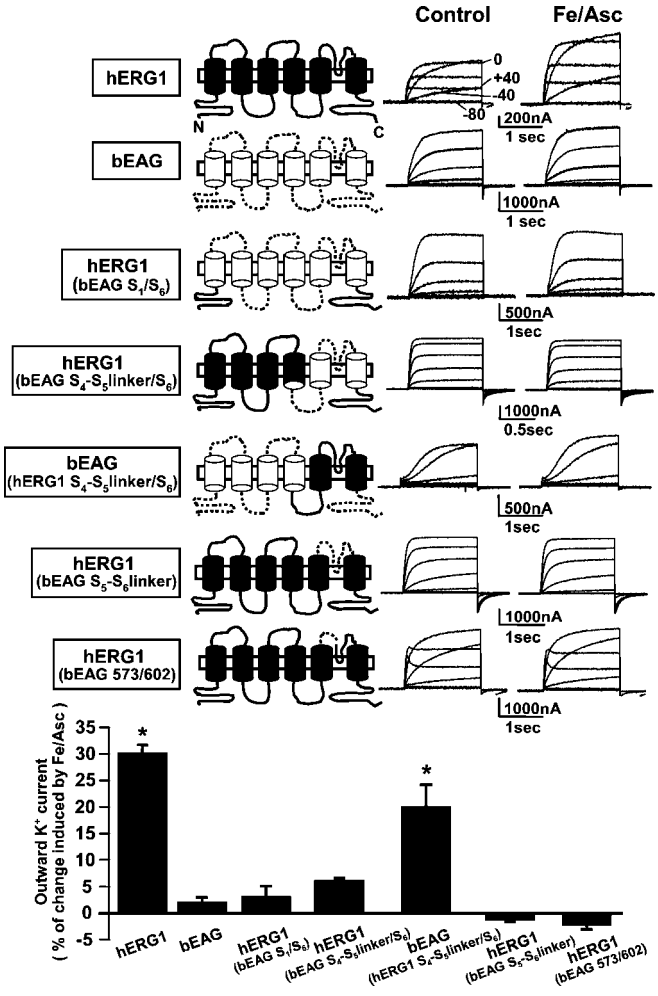

FIG. 1. **Effect of Fe/Asc perfusion on the K^+ channels encoded by *hERG1*, *bEAG*, and *hERG1/bEAG* chimeras expressed in *Xenopus* oocytes.** Representative current traces. Individual oocytes expressing hERG1, bEAG, hERG1 (bEAG S_1/S_6), hERG1 (bEAG S_4-S_5 linker/S_6), bEAG (hERG1 S_4-S_5 linker/S_6), hERG1 (bEAG S_5-S_6 linker), or hERG1 (bEAG 573/602) chimeric channels were studied in control conditions and after Fe/Asc exposure (25 μM $FeSO_4$ and 50 μM ascorbate). Holding potential: −90 mV; depolarizing steps from −80 to +40 mV (for hERG1, bEAG, hERG1 (bEAG S_4-S_5 linker/S_6), hERG1 (bEAG S_5-S_6 linker), and hERG1 (bEAG 573/602)), or from −80 to +20 mV (for hERG1(bEAG S_1/S_6) and bEAG (hERG1 S_4-S_5 linker/S_6)) in 20 mV increments; return potential: −100 mV. *Next to each set of traces*, a schematic drawing showing a single K^+ channel subunit, represented as a six-transmembrane domain protein with intracellular amino and the carboxyl termini, and the chimeric regions exchanged between hERG1 (*black* with *thick lines*) and bEAG (*white* with *dotted lines*) are shown. *Bottom*, a summary of the effect of a 5-min perfusion with Fe/Asc on the outward K^+ currents carried by the different channels investigated is shown. On the *ordinate* is reported the percentage of variation induced by the Fe/Asc perfusion on the outward K^+ currents carried by each channel, obtained by measuring the currents at the end of a depolarizing pulse to potentials, which fully activated the conductance (+20 or +40 mV) after Fe/Asc treatment. This value is expressed as a percentage of that recorded before Fe/Asc exposure. Each column is the mean ± S.E. of the results obtained in four to eight cells. *Asterisks* denote values significantly different from control values ($p < 0.05$).

solution (25 and 50 μM, respectively) increased by ~30% hERG1 outward K^+ currents evoked by depolarizing steps from −80 mV to +40 mV from a holding voltage of −90 mV (Fig. 1). The increase of hERG1 outward current induced by Fe/Asc was independent on extracellular K^+ concentrations ($[K^+]_e$), because it was observed with $[K^+]_e$ ranging from 2 (data not shown) to 42 mM; with 42 mM $[K^+]_e$, the outward currents at 0 mV were increased by 26 ± 9% in the presence of Fe/Asc ($p > 0.05$ *versus* that observed with 10 mM $[K^+]_e$; $n = 5$). By contrast, the K^+ channels encoded by bEAG gave rise to delayed rectifier-like outward currents with activation kinetics strongly dependent on the holding potential and an extremely fast current deactivation at more hyperpolarized membrane potentials. Interestingly, the currents carried by bEAG channels were completely insensitive to Fe/Asc perfusion (Fig. 1), suggesting therefore that bEAG channels are resistant to ROS-induced modulation.

To localize the molecular regions involved in ROS-induced modulation of hERG1 K^+ channels, we took advantage of the fact that the bEAG K^+ channels were insensitive to ROS; thus, segmental exchanges between hERG1 and bEAG K^+ channel subunits were performed. Replacement of the "core" region (from the beginning of S_1 to the end of S_6) of hERG1 with the corresponding region of bEAG (chimeric construct hERG1 (bEAG S_1/S_6)), led to the expression of K^+-selective channels that were insensitive to Fe/Asc perfusion. Similarly, exchange of the region spanning from the beginning of the S_4-S_5 linker to the end of S_6 of hERG1 with the corresponding region of bEAG (hERG1 (bEAG S_4-S_5 linker/S_6)), also led to the disappearance of the channel sensitivity to ROS. Interestingly, the reverse chimeric exchange, namely the replacement of the region between the beginning of the S_4-S_5 linker region to the end of S_6 of bEAG with the corresponding hERG1 sequence (bEAG (hERG1 S_4-S_5 linker/S_6)), generated channels having K^+ currents that were significantly potentiated by Fe/Asc perfusion (Fig. 1). These results suggested that the ROS-induced modulation of hERG1 K^+ channels required the presence of a specific amino acid sequence in the region located between the S_4-S_5 linker and the S_6 transmembrane domain. Within this region, a smaller chimera substituting only the S_5-S_6 linker of hERG1 with that of bEAG (hERG1 (bEAG S_5-S_6 linker)) generated K^+ channels that were still insensitive to Fe/Asc-induced modulation, suggesting that the molecular determinants for ROS sensitivity of hERG1 are located within the S_5-S_6 linker. To more specifically localize the amino acids involved in ROS sensitivity within the S_5-S_6 linker region of hERG1, a smaller chimera (hERG1 (bEAG 573/602)) was generated. In this construct, a 30-amino acid sequence of hERG1 (from the end of the putative S_5 transmembrane segment to the GGPS amino acid sequence present in both hERG1 and bEAG) was substituted with the corresponding 40-amino acid stretch encoded by bEAG (Fig. 2). The K^+ channels encoded by this chimeric construct were completely insensitive to the effects of Fe/Asc (25/50 μM) perfusion (Fig. 1), supporting the idea that residues located within this 30-amino acid sequence of hERG1 are crucially involved in determining the channel sensitivity to ROS.

The currents carried by the hERG1 (bEAG 573/602) chimera displayed a selectivity for K^+ ions identical to that of wild-type hERG1 channels. With 10 mM K^+ ions in the extracellular solution, the reversal potential for the currents carried by wild-type hERG1 channels was −60 ± 0.6 mV ($n = 6$), whereas that for hERG1 (bEAG 573/602) channels was −57.6 ± 1.6 mV ($n = 5$) ($p > 0.05$). Furthermore, the midpoint voltage of channel activation and the slope of the activation curves, calculated as described in the legend for Fig. 3, were, respectively: −32.4 ± 1.07 mV and 8.77 ± 0.8 ($n = 4$) for wild-type hERG1 and −31.75 ± 1.5 mV and 8.1 ± 0.43 ($n = 4$) for hERG1 (bEAG 573/602) ($p > 0.05$). Interestingly, the midpoint voltage of channel inactivation was significantly affected by the mutation, because it was −61.8 ± 1.0 mV ($n = 13$) for wild-type hERG1 and −68.5 ± 0.6 mV ($n = 4$) for hERG1 (bEAG 573/602) ($p < 0.05$). The slopes of the inactivation curves were, respectively, 17.3 ± 0.3 mV and 18.0 ± 0.7 ($p > 0.05$) for the two channels (Fig. 3*A*).

In addition, the currents carried by the hERG1 (bEAG 573/602) chimeric channels were insensitive not only to perfusion

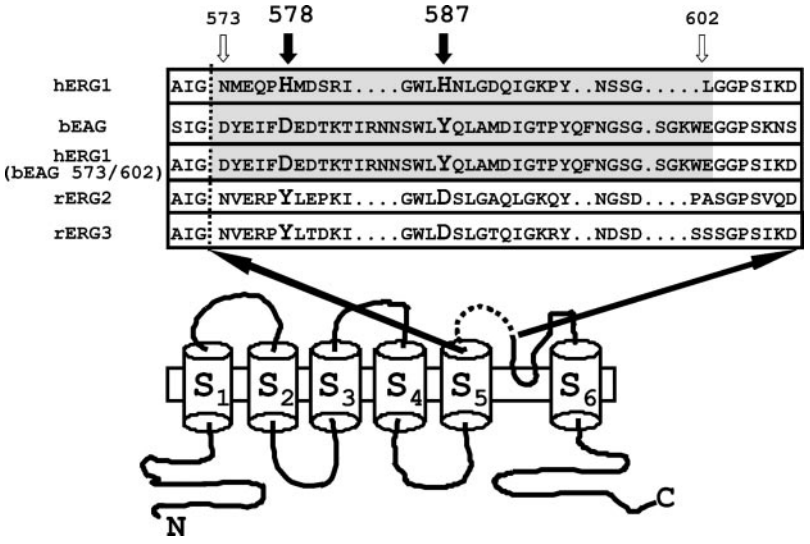

FIG. 2. **Alignment of the region of the S_5-S_6 linker region encompassed by the hERG1 (bEAG 573/602) chimera.** The *single-letter abbreviation code* has been adopted to indicate amino acid residues. *Dots* indicate gaps in the sequence introduced by the software used to generate the alignment (ClustalW, version 1.6, EMBL Heidelberg, Germany). The *shaded area* of the amino acid sequence corresponds to the chimeric region encompassed by the hERG1 (bEAG 573/602) chimera. The amino acids at positions 573 and 602 in the hERG1 sequence, representing the beginning and the end of the chimeric region, respectively, are indicated by the *empty arrows*. The two histidines at positions 578 and 587 in the hERG1 sequence are indicated by the *filled arrows*.

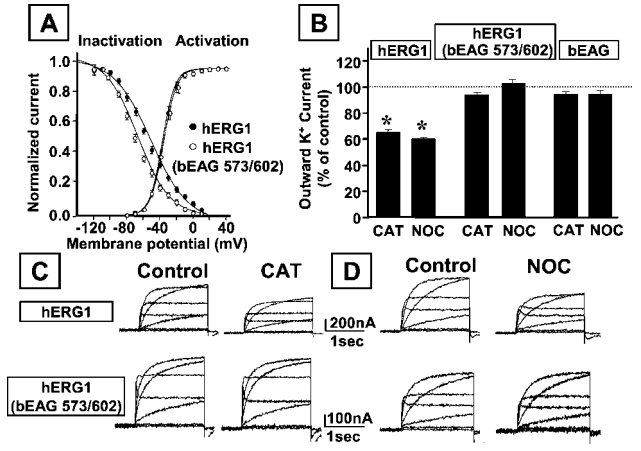

FIG. 3. **Effect of catalase (*CAT*) and DETA NONOate (*NOC*) on hERG1, bEAG, and hERG1 (bEAG 573/602) chimeric channels expressed in *Xenopus* oocytes.** *A*, steady-state activation and inactivation properties of hERG1 (bEAG 573/602) chimeric channels. To measure the voltage dependence of activation, the following voltage protocol was used: holding potential −90 mV, 1.75-s depolarizing steps from −80 to +30 mV in 10-mV increments, return potential −100 mV. The currents recorded upon repolarization to −100 mV were measured, normalized to the maximum value, and plotted *versus* the membrane voltage of the depolarizing step. For the inactivation curves, the following voltage protocol was used: holding potential −90 mV, 1.75-s depolarizing steps to 0 mV, 25-ms conditioning pulses from −120 mV to +60 mV in 10-mV increments, and 200-ms test potential to +20 mV. The initial currents recorded immediately after delivering the +20-mV test pulse were measured, normalized to the maximum value, and plotted *versus* the membrane voltage of the conditioning pulses. The experimental data were fitted to the following form of the Boltzmann equation: $gK_v = \max/(1 + \exp(V_{½} - V)/k)$, where V is the test potential, $V_{½}$ is the half-activation potential, and k (or kT/ze) is the slope of the conductance to voltage relationship. *B*, quantification of the effect of CAT and NOC on the outward currents carried by hERG1, hERG1 (bEAG 573/602), or bEAG channels. The same oocytes expressing the channel of interest were recorded in control condition and after 5-min exposure to CAT (1000 units/ml) or NOC (0.3 mM). The outward K^+ currents were measured at the end of 1.75-s depolarizing pulses to 0 mV (or +40 mV for bEAG) after the exposure to different experimental conditions and expressed as a percentage of the respective control value. *C* and *D*, representative traces recorded from oocytes expressing hERG1 or hERG1 (bEAG 573/602) chimeric channels recorded in control conditions and after 5-min exposure to 1000 units/ml CAT (*C*) or 0.3 mM NOC (*D*). The voltage protocol is identical to that described in Fig. 1.

with Fe/Asc but also with the ROS-detoxifying enzyme catalase (1000 units/ml) (Fig. 3*B*); furthermore, the same chimeric substitution also removed the channel sensitivity to the NO·-donor NOC (0.3 mM) (Fig. 3*B*). Fig. 3 (*C* and *D*) shows the effects of a 5-min perfusion with catalase and NOC, respectively, on the outward K^+ currents carried by the channels encoded by wild-type hERG1 and hERG1 (bEAG 573/602).

Given the results obtained with the hERG1 (bEAG 573/602) chimera, we engineered a reverse chimeric exchange by transplanting the hERG1 573–602 region into bEAG, to investigate whether this chimeric replacement was sufficient to introduce ROS modulation into ROS-insensitive bEAG channels. Unfortunately, injection of *Xenopus* oocytes with the cRNA encoded by this chimeric cDNA construct did not lead to the expression of functional channels (data not shown).

Effect of Mutations of the Histidine Residues at Positions 578 and 587 in hERG1 on the Current Modulation by ROS and RNS in Xenopus Oocytes—The results presented showed that the 30-amino acid region in the S_5-S_6 linker of hERG1 channels substituted in the hERG1 (bEAG 573/602) chimera contains the molecular determinants responsible for the channel sensitivity to ROS-induced modulation. As shown in the alignment of Fig. 2, within this 30-amino acid region, the hERG1 sequence contains two histidines at position 578 and 587, which are not present in the ROS-insensitive bEAG, rERG2, and rERG3 K^+ channels. Therefore, the possible involvement of these two histidine residues in the modulation of hERG1 channels by ROS was investigated.

As shown in Fig. 4, single point mutations at positions 578 or 587 introducing in hERG1 the corresponding bEAG residues (hERG1 H578D and hERG1 H587Y), as well as the double-substitution hERG1 H578D/H587Y, completely removed the channel sensitivity to the stimulatory effect exerted by Fe/Asc (25/50 μM, respectively). In addition, the inhibition of the outward hERG1 K^+ currents caused by catalase (1000 units/ml) and by the NO· donor NOC (0.3 mM) was completely abolished in these histidine-lacking mutant channels.

The removal of each of the two histidines caused a leftward shift in the channel voltage dependence of inactivation, without affecting the activation process. In fact, the midpoint voltage of channel activation and the slope of the activation curves were, respectively, −35 ± 0.3 mV and 9.18 ± 0.2 (n = 8) for wild-type hERG1, −37 ± 0.19 mV and 9.1 ± 0.04 (n = 6) for hERG1 H578D, −35.2 ± 0.77 mV and 9.13 ± 0.09 (n = 6) for hERG1 H587Y, and −37 ± 0.6 mV and 8.6 ± 0.08 (n = 7) for hERG1 H578D/H587Y ($p > 0.05$). On the other hand, the midpoint voltage of channel inactivation and the slope of the inactivation curves were, respectively, −61.8 ± 1.0 mV and 17.3 ± 0.3 (n = 13) for wild-type hERG1, −87.1 ± 1.8 mV ($p <$ 0.05 *versus* hERG1) and 20 ± 0.8 (n = 7) for hERG1 H578D,

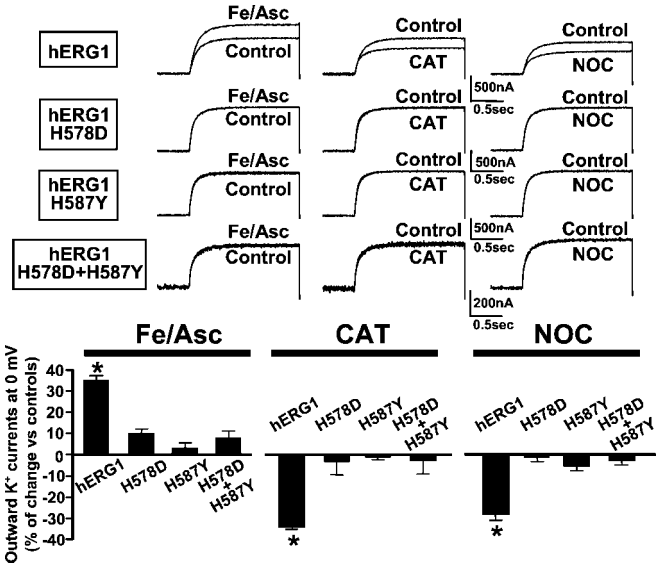

FIG. 4. **Effect of Fe/Asc, CAT, and NOC on the currents carried by wild-type hERG1 and hERG1 mutants H578D, H587Y, and H578D/H587Y expressed in *Xenopus* oocytes.** The *top part* of the figure shows superimposed representative current traces recorded from individual cells expressing the different channels exposed to control conditions and after 5-min perfusion with Fe/Asc (25 and 50 μM, respectively), CAT (1000 units/ml), or NOC (0.3 mM). Test potential: 0 mV; holding voltage: −90 mV. In the *bottom part*, the *columns* represent the mean ± S.E. of the results obtained for each experimental treatment in four to eight cells, quantified as described in Fig. 1. Double mutants are represented by the "+" symbol.

−69.0 ± 1.2 mV ($p < 0.05$ *versus* hERG1) and 17.4 ± 0.5 ($n = 7$) for hERG1 H587Y, and −72.2 ± 0.7 mV ($p < 0.05$ *versus* hERG1) and 15.3 ± 0.2 ($n = 6$) for hERG1 H578D/H587Y.

Molecular Mechanism for the Involvement of hERG1 Histidines at Position 578 and 587 in ROS- and RNS-induced Channel Modulation—To gain more insight into the molecular mechanism by which histidines at position 578 and 587 participate in hERG1 channel modulation by ROS, the possible involvement of iron ions has also been investigated. To this aim, the effect exerted on hERG1 channels by the two iron chelators desferrioxamine (DFX) (6, 30) and *o*-phenanthroline (PHE) (31), were studied. Perfusion of hERG1-expressing oocytes for 5 min with DFX (1 mM) or PHE (0.2 mM) significantly inhibited the outward K^+ currents at all the potentials tested between −40 and +40 mV (Fig. 5*A*), without affecting either the amplitude or the kinetics of the inward currents (data not shown). Interestingly, the inhibitory effect of DFX on hERG1 currents was not reversible upon washout of the iron chelator from the perfusion medium for up to 20 min; however, the presence of 25 μM $FeSO_4$ (with or without 50 μM ascorbic acid) readily increased hERG1 outward currents back to their resting value (Fig. 5*B*). These results suggest that the inhibition of hERG1 outward K^+ currents by DFX was due to the drug ability to specifically chelate iron ions, rather than being the consequence of an unspecific effect of the molecule or its ability to chelate other metal ions, which are known to influence hERG1 channel function (32). Furthermore, DFX (1 mM) completely counteracted the stimulatory effect of Fe/Asc (25/50 μM) on the outward K^+ currents carried by hERG1 (Fig. 5*C*). Interestingly, DFX (1 mM) was also able to prevent the inhibitory action of the ROS-detoxifying enzyme catalase (1000 units/ml) on hERG1 outward K^+ currents under resting conditions (Fig. 5*D*).

To test more directly the hypothesis that the iron chelators DFX and PHE might interfere with the oxidating process promoted by iron ions, the effects of DFX and PHE on resting and Fe/Asc-enhanced intracellular malondialdehyde (MDA) production, a direct index of lipid peroxidation, were measured. Both DFX (0.1–1 mM) and PHE (0.2 mM) effectively decreased the basal concentration of MDA (Fig. 6). Furthermore, DFX (1 mM) was able to prevent the Fe/Asc-induced increase in MDA production, confirming that, in the presence of the iron chelator, iron ions are unable to participate in the Fenton reaction and to trigger oxidative stress.

Effect of DFX and PHE on hERG1 Channels Lacking Histidines at Positions 578 and 587—To investigate the possible participation of hERG1 histidines at position 578 and 587 in iron-dependent channel modulation by ROS, the effects of the iron chelators DFX and PHE on the histidine-lacking channels hERG1 H578D/H587Y and bEAG were compared with those occurring in wild-type hERG1 channels. Both DFX (1 mM) and PHE (0.2 mM) were without any effect in the hERG1 mutant H578D/H587Y; furthermore, bEAG channels were unaffected by both DFX (1 mM) and PHE (0.2 mM) (Fig. 7).

DISCUSSION

Previous studies have shown that the currents carried by heterologously expressed hERG1 K^+ channels are regulated by ROS. In fact, increasing the production of more reactive ROS by perfusion with Fe/Asc, an experimental condition widely used to trigger oxidative stress (1), enhanced hERG1 outward K^+ currents heterologously expressed in *Xenopus* oocytes. On the other hand, the reduction of basal ROS production by catalase caused a marked inhibition of hERG1 outward K^+ currents in resting conditions and prevented their stimulation by Fe/Asc (22). More recently, an increase in hERG1 outward currents has also been found in *hERG1*-transfected Chinese hamster ovary cells exposed to H_2O_2, an oxidative stimulus analogous to Fe/Asc (33). In addition, both endogenously produced and pharmacologically delivered $NO^{\cdot}$ exerts an inhibitory effect on resting hERG1 outward K^+ currents and prevents their enhancement triggered by Fe/Asc (23). These results were interpreted as a consequence of the ability of $NO^{\cdot}$ to interact with ROS species generated in resting conditions or produced by Fe/Asc perfusion, suggesting a potent antioxidant effect of this gaseous mediator (24, 34, 35). The biophysical mechanism by which changes in ROS affected hERG1 K^+ channel function seems to be a result of the interference of such changes with the hERG1 fast inactivation process, which reduces the conductance at positive membrane potentials and leads to an inwardly rectifying current-to-voltage relationship (17, 25). Increased ROS production caused a rightward shift of the voltage dependence of inactivation, whereas a decrease of ROS shifted the channel voltage dependence of inactivation in the leftward direction (22).

In the present study, by means of chimeric exchanges between the ROS-sensitive channel hERG1 and the ROS-insensitive channel bEAG, the identification of the molecular determinants responsible for hERG1channel modulation by ROS has been pursued. The results obtained with the chimeric constructs hERG1(bEAG S_1/S_6), hERG1 (bEAG S_4-S_5 linker/S_6), and hERG1 (bEAG S_5-S_6 linker), in which progressively smaller regions of the core sequence of hERG1 were substituted with the corresponding regions of bEAG, support the S_5-S_6 linker as a crucial determinant for hERG1 ROS sensitivity. Interestingly, a reverse chimeric exchange replacing the bEAG region from the beginning of the S_4-S_5 linker region to the end of S_6 with the corresponding hERG1 sequence (bEAG (hERG1 S_4-S_5 linker/S_6) introduced ROS sensitivity into bEAG channels. However, the K^+ channels generated by the three chimeric exchanges introducing bEAG sequences into hERG1 displayed outwardly rectifying current-to-voltage relationships, suggesting a loss in the fast inactivation process. These results raise the possibility that the insensitivity to ROS modulation

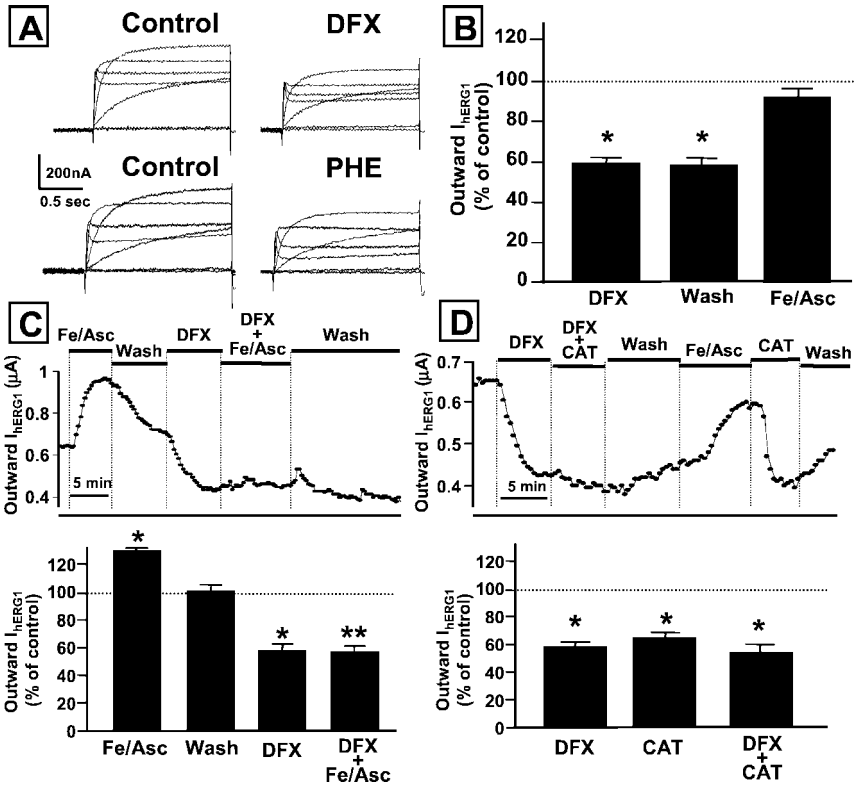

FIG. 5. **Effect of DFX and PHE on basal, Fe/Asc-enhanced, and CAT-inhibited hERG1 K^+ currents in *Xenopus* oocytes.** *A*, effect of DFX (1 mM) and PHE (0.2 mM) on hERG1 outward K^+ currents. Outward K^+ current traces recorded from hERG1 channels in control conditions and after 5-min exposure to 1 mM DFX or 0.2 mM PHE are shown. The currents were evoked by 1.75-s depolarizing pulses from −80 mV to +40 mV in 20-mV increments from a holding potential of −90 mV. The inward current component elicited upon repolarization to −100 mV has been *omitted* for clarity. *B*, effect of DFX (1 mM) and of the subsequent washout with DFX-free solution and perfusion with Fe/Asc on hERG1 outward K^+ currents. The outward hERG1 K^+ currents measured at the end of 1.75-s depolarizing pulses to 0 mV after 5-min exposure to DFX (1 mM), then subsequent 10-min washout with DFX-free solution (*Wash*) followed by Fe/Asc (25 and 50 μM, respectively), are expressed as percentage of the control current recorded at the beginning of the experiment. *Asterisks* denote values significantly different from control values ($p < 0.05$). *C* and *D*, effect of DFX on the Fe/Asc-induced enhancement of hERG1 outward K^+ currents (*C*) and on the CAT-induced inhibition of hERG1 outward K^+ currents (*D*). The *top part of each panel* shows a time course of the outward hERG1 K^+ currents, measured at the end of repetitive depolarizing pulses to 0 mV elicited every 20 s, during the exposure to the indicated experimental conditions in a representative cell. In the *bottom part of the panels*, the *columns* represent the mean ± S.E. of the results obtained for each experimental treatment in four to eight cells. hERG1 outward K^+ currents were measured at the end of the exposure to each experimental condition and expressed as percentage of the control current recorded at the beginning of the experiment.

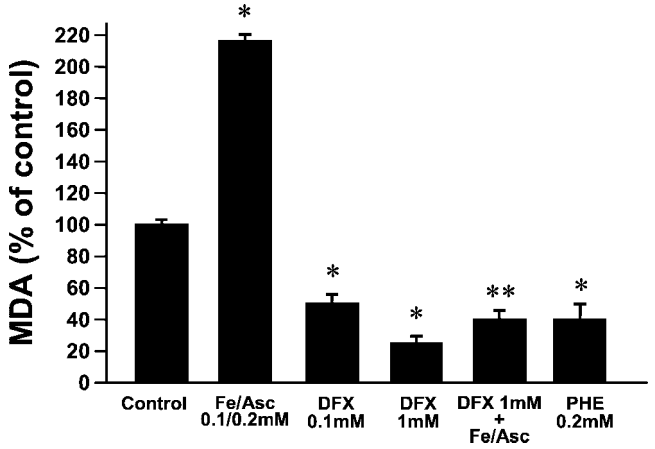

FIG. 6. **Effects of DFX and PHE on resting and Fe/Asc-induced lipid peroxidation in *Xenopus* oocytes.** Each *column* is the mean ± S.E. of 4–16 determinations performed in triplicate. *Asterisks* denote values significantly different from control values ($p < 0.05$). *Double asterisks* indicate values significantly different from the Fe/Asc group ($p < 0.05$). The MDA content in the control group was 6.7 ± 0.9 pmol/mg of protein/2 h.

shown by these chimeras was possibly caused not only by the removal of specific amino acids participating in ROS modulation but also by the lack of the inactivation process. A solution to this issue came from the experiments performed with the smaller chimeric exchange named hERG1 (bEAG 573/602), which only encompassed 30 amino acids in the S_5-S_6 linker of hERG1 immediately past the S_5 putative transmembrane segment. The K^+ currents encoded by this chimeric construct mainly retained the biophysical and pharmacological properties of hERG1 channels; in fact, the chimeric channels encoded by hERG1 (bEAG 573/602), in a manner similar to wild-type hERG1 channels, displayed strong inward rectification at positive membrane potential and high affinity block by the class III antiarrhythmic dofetilide (29). However, this small chimeric substitution caused a complete loss in the sensitivity to ROS, as suggested by the observation that the current carried by the hERG1 (bEAG 573/602) chimera was resistant not only to ROS exogenously generated by Fe/Asc but also to the decrease of constitutive ROS levels achieved with the ROS-detoxifying enzyme catalase. The removal of the effect of extracellularly perfused catalase in the hERG1 (bEAG 573/602) chimera is compatible with the idea that the chimeric region responsible for ROS sensitivity in hERG1 is located extracellularly, a view consistent with the available K^+ channels structural data (36). Furthermore, the fact that the hERG1 (bEAG 573/602) chimeric channels were also insensitive to the $NO^{\cdot}$ donor NOC confirms that $NO^{\cdot}$ modulated hERG1 outward currents indirectly, possibly by scavenging ROS produced under resting condition or during oxidative stress (23).

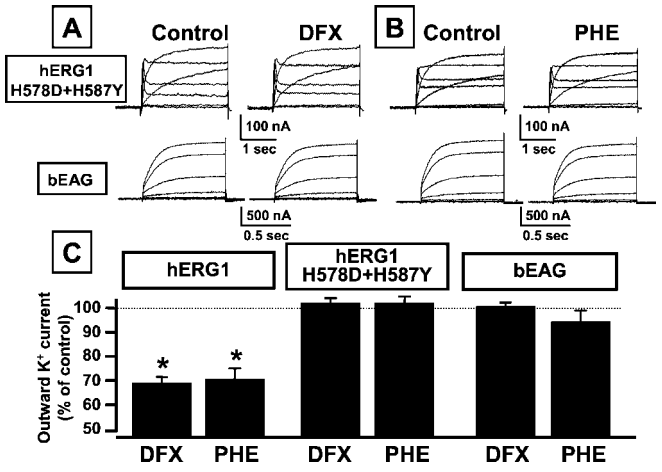

FIG. 7. **Effect of DFX and PHE on the outward currents carried by the hERG1 H578D/H587Y and bEAG K^+ channels.** *A* and *B*, outward K^+ current traces recorded from representative oocytes expressing the hERG1 H578D/H587Y mutant or bEAG exposed to control conditions and after 5-min exposure to 1 mM DFX (*A*) or 0.2 mM PHE (*B*). The currents were evoked by depolarizing pulses from −80 mV to +40 mV in 20-mV increments from a holding potential of −90 mV. The inward current component elicited upon repolarization to −100 mV has been *blanked* for clarity in the traces corresponding to the hERG1 H578D/H587Y mutant. *C*, effect of DFX and PHE on the outward currents carried by hERG1, hERG1 H578D/H587Y, and bEAG. The columns represent the mean ± S.E. of the effect exerted by DFX (1 mM) and PHE (0.2 mM) in four to eight oocytes expressing the different K^+ channels. The outward currents, measured at the end of the depolarizing pulses to 0 mV (for hERG1 and hERG1 H578D/H587Y) or +40 mV (for bEAG) were expressed as percentage of the respective currents recorded before drug application.

Within the 30-amino acid region encompassed by the hERG1 (bEAG 573/602) chimera, two histidines are present in hERG1 sequence at positions 578 and 587. These two histidine residues are peculiar of hERG1 sequence, because different amino acids are present at corresponding positions in the primary sequences of other K^+ channel subunits closely related to hERG1, such as bEAG, rERG2, and rERG3 (Fig. 2). Interestingly, these latter K^+ channels lack ROS sensitivity (22, 23). This observation, together with the fact that histidines are among the preferential targets for ROS-induced modifications of protein function during oxidative stress (11), prompted us to perform experiments in which single-point mutations were introduced to substitute these two histidines with the corresponding bEAG amino acids. The results obtained suggested that the K^+ channels encoded by the hERG1 mutants H578D, H587Y, and H578D/H587Y lost the sensitivity to both the stimulatory effect of Fe/Asc-induced ROS formation and to the inhibitory effect of catalase. Interestingly, all three mutant channels were also refractory to the inhibition by $NO^\cdot$ donors. These experiments clearly highlighted the participation of both histidines in such important modulatory mechanism. On the other hand, these two histidines seem not to be involved in hERG1 sensitivity to extracellular pH changes (32, 37–40). Interestingly, the histidine-lacking hERG1 channels displayed a leftward shift in the voltage dependence of channel inactivation resembling that produced in wild-type hERG1 channels by catalase and $NO^\cdot$-donors; this result is consistent with the idea that oxidative modification of these histidines underlie hERG1 channel modulation by oxidative stress.

Given that endogenously present or exogenously delivered iron ions participate in the Fenton reaction leading to ROS production, hERG1 K^+ currents modulation by the two iron chelators DFX, which is unable to significantly enter the cell by passive diffusion (6, 30), and PHE, which shows significant intracellular penetration (31), was also investigated. Both compounds, despite having different chemical structures, significantly inhibited resting outward K^+ currents carried by wild-type hERG1 channels, suggesting that DFX- or PHE-chelated iron ions are unable to participate in the Fenton reaction modulating hERG1 channels during oxidative stress. These results also suggested that endogenous iron ions are possibly involved in controlling resting ROS production, which, in turn, modulate hERG1 channel function. This view seems to be supported by the experiments showing that DFX and PHE were able to reduce lipid peroxidation in resting conditions. The important role played by endogenous iron ions in maintaining tonic production of ROS is also suggested by the observation that the inhibitory effect exerted on hERG1 outward K^+ currents by DFX and catalase were not additive, a result possibly explained by the fact that the removal of either substrates participating in the Fenton reaction (either Fe^{2+} by DFX or H_2O_2 by catalase) during both resting and oxidative stress did not produce a further inhibition of hERG1 outward K^+ currents. In keeping with these results, DFX was also able to completely prevent the increase in both lipid peroxidation and hERG1 outward K^+ currents induced by Fe/Asc.

The results presented suggested that endogenous iron ions have an important role in modulating the sensitivity of wild-type hERG1 K^+ channels to ROS. Considering that histidines at positions 578 and 587 in hERG1 channels are involved in ROS sensitivity, and in view of the fact that histidines in proteins are often associated with transition metals (12), we studied the effects of DFX and PHE on hERG1 mutant channels in which both histidines had been replaced with the corresponding bEAG residues. In the hERG1 H578D/H587Y mutant, as in wild-type bEAG, DFX and PHE failed to modify the outward K^+ currents recorded in basal conditions. These results suggested that histidines in the S_5-S_6 linker are crucial players in iron-dependent ROS production modulating hERG1 K^+ channel function. However, although the present experiments do not definitively describe the molecular mechanism by which these aromatic amino acids participate in such modulation, two hypothesis can be made. The first hypothesis suggests that histidines at position 578 and 587 of hERG1 may be involved in the coordination of iron ions participating in the production of ROS, which would affect channel function at sites different from histidines themselves. Another possible speculation implies that these histidines may represent direct molecular targets for ROS action. In our view, the latter hypothesis seems more likely given that the histidine-lacking hERG1 H578D/H587Y mutant was also resistant to the modulation by exogenous ROS generated upon extracellular exposure to Fe/Asc. On the other hand, it should be emphasized that these two mechanisms might not be mutually exclusive, because histidines might be sites for both iron coordination and ROS action. This latter possibility has already been shown to occur in human growth hormone, where oxidative stress *in vitro* triggers the oxidation to 2-oxo-histidine of two histidine residues located in the metal-binding site of the molecule (41).

Changes in the excitability of cardiac and neuronal cells triggered by variations in ROS and RNS concentrations are crucial determinants of cellular responses during ischemia-reperfusion events (14, 42), and voltage-dependent K^+ channels appear to play a major role in such responses (15, 43). hERG1 K^+ channels underlie the rapid component of the cardiac repolarizing current I_{Kr}. The present results, showing that iron-dependent basal ROS and $NO^\cdot$ production tonically regulate hERG1 outward currents, although they are obtained in an amphibian heterologous expression system to avoid perturbation of the intracellular environment and contamination by overlapping currents, might be of crucial pathophysiological

relevance considering that oxidative damage shortened the action potential duration in Purkinje fibers (44, 45) and in ventricular myocytes after prolonged times of exposure to ischemia-reperfusion conditions (46, 47). Furthermore, the present results might represent a novel mechanism linking changes in iron levels, which occur in the coronary flow during global ischemia followed by reperfusion (48) and promote an increased production of toxic $^{\bullet}OH$ radicals (6), with the described electrophysiological changes at the myocardial level. Also in the brain, the acidosis that accompanies the ischemic insult results in an increased release of iron ions from its cellular storage sites (49), and iron-chelating agents are known to provide protection from the ischemic damage both *in vitro* (50) and *in vivo* (6). Finally, in rat hippocampus, *ERG1* transcripts are abundantly expressed in parvalbumin-positive interneurons (51), a cell population resistant to ischemia (52); on the other hand, CA1 pyramidal neurons, which are highly vulnerable to ischemia, express low levels of *ERG1* and high levels of *ERG3* transcripts, the latter encoding for ROS-insensitive subunits. These observations make possible the hypothesis that the described modulation of ERG1 K^+ channels by iron-dependent ROS production might participate in the selective survival of hippocampal interneurons during ischemic insults.

Acknowledgments—We are indebted to Drs. M. T. Keating (Salt Lake City, UT) for hERG1 cDNA and A. Baumann (Jülich, Germany) for bEAG cDNA.

REFERENCES

1. Yu, B. P. (1994) *Physiol. Rev.* **74,** 139–162
2. Kaneko, M., Matsumoto, Y., Hayashi, H., Kobayashi, A., and Yamazaki, N. (1994) *Mol. Cell. Biochem.* **139,** 91–100
3. Coyle, J. T., and Puttfarcker, P. (1993) *Science* **262,** 689–695
4. Sohal, R. S., and Weindruch, R. (1996) *Science* **273,** 59–63
5. Korsmeyer, S. J., Yin, X. M., Oltvai, Z. N., Veis-Novak, D. J., and Linette, G. P. (1995) *Biochim. Biophys. Acta* **1271,** 63–66
6. Halliwell, B., and Gutteridge, J. M. C. (1989) in *Free Radicals in Biology and Medicine*, 2nd Ed., Clarendon Press, Oxford, pp. 1–81
7. Halliwell, B. (1992) *J. Neurochem.* **59,** 1609–1623
8. Gross, S. S., and Wolin, M. S. (1995) *Annu. Rev. Physiol.* **57,** 737–769
9. Darley-Usmar, V., Wiseman, H., and Hallywell, B. (1995) *FEBS Lett.* **369,** 131–135
10. Iadecola, C. (1997) *Trends Neurosci.* **20,** 132–139
11. Stadtman, E. R. (1993) *Annu. Rev. Biochem.* **62,** 797–821
12. Chevion, M. (1988) *Free Radic. Biol. Med.* **5,** 27–37
13. Uchida, K., and Kawakishi, S. (1993) *FEBS Lett.* **332,** 208–210
14. Martin, R. L., Lloyd, H. G., and Cowan, A. I. (1994) *Trends Neurosci.* **17,** 251–257
15. Kourie, J. I. (1998) *Am. J. Physiol.* **275,** C1–C24
16. Warmke, J. W., and Ganetzky, B. (1994) *Proc. Natl. Acad. Sci. U. S. A.* **91,** 3438–3442
17. Sanguinetti, M. C., Jiang, C., Curran, M. E., and Keating, M. T. (1995) *Cell* **81,** 299–307
18. Curran, M. E., Splawski, I., Timothy, K. W., Vincent, G. M., Green, E. D., and Keating, M. T. (1995) *Cell* **80,** 795–803
19. Arcangeli, A., Bianchi, L., Becchetti, A., Faravelli, L., Coronnello, M., Mini, E., Olivotto, M., and Wanke, E. (1995) *J. Physiol. (Lond.)* **489,** 455–471
20. Faravelli, L., Arcangeli, A., Olivotto, M., and Wanke, E. (1996) *J. Physiol. (Lond.)* **469,** 13–23
21. Chiesa, N., Rosati, B., Arcangeli A., Olivotto, M., and Wanke, E. (1997) *J. Physiol. (Lond.)* **501,** 313–318
22. Taglialatela, M., Castaldo, P., Iossa, S., Pannaccione, A., Fresi, A., Ficker, E., and Annunziato, L. (1997) *Proc. Natl. Acad. Sci. U. S. A.* **94,** 11698–11703
23. Taglialatela, M., Pannaccione, A., Castaldo, P., Iossa, S., and Annunziato, L. (1999) *Mol. Pharmacol.* **56,** 1298–1308
24. Kanner, J., Harel, S., and Granit, R. (1991) *Arch. Biochem. Biophys.* **289,** 130–136
25. Smith, P. L., Baukrowitz, T., and Yellen, G. (1996) *Nature* **379,** 833–836
26. Shi, W., Wymore, R. S., Wang, H. S., Pan, Z., Cohen, I. S., McKinnon, D., and Dixon, J. E. (1997) *J. Neurosci.* **17,** 9423–9432
27. Esterbauer, H., and Cheeseman, K. H. (1990) *Methods Enzymol.* **186,** 407–421
28. Frings, S., Brull, N., Dzeja, C., Angele, A., Hagen, V., Kaupp, U. B., and Baumann, A. (1998) *J. Gen. Physiol.* **111,** 583–599
29. Ficker, E., Jarolimek, W., Kiehn, J., Baumann, A., and Brown, A. M. (1998) *Circ. Res.* **82,** 386–395
30. Lloyd, J. B., Cable, H., and Rice-Evans, C. (1991) *Biochem. Pharmacol.* **41,** 1361–1363
31. Boumans, H., van Gaalen, M. C., Grivell, L. A., and Berden, J. A. (1997) *J. Biol. Chem.* **272,** 16753–16760
32. Ho, W. K., Kim, I., Lee, C. O., Youm, J. B., Lee, S. H., and Earm, Y. E. (1999) *Biophys. J.* **76,** 1959–1971
33. Bérubé, J., Caouette, D., and Daleau, P. (2001) *J. Pharmacol. Exp. Ther.* **297,** 96–102
34. Rubbo, H., Radi, R., Trujillo, M., Telleri, R., Kalyanaraman, B., Barnes, S., Kirk, M., and Freeman, B. A. (1994) *J. Biol. Chem.* **269,** 26066–26075
35. Goss, S. P., Kalyanaraman, B., and Hogg, N. (1999) *Methods Enzymol.* **301,** 444–453
36. Doyle, D. A., Morais Cabral, J., Pfuetzner, R. A., Kuo, A., Gulbis, J. M., Cohen, S. L., Chait, B. T., and MacKinnon, R. (1998) *Science* **280,** 69–77
37. Bérubé, J., Chahine, M., and Daleau, P. (1999) *Pflugers Arch.* **438,** 419–422
38. Jiang, M., Dun, W., and Tseng, G. N. (1999) *Am. J. Physiol.* **277,** H1283–H1292
39. Jo, S. H., Youm, J. B., Kim, I., Lee, C. O., Earm, Y. E., and Ho, W. K. (1999) *Pflugers Arch.* **438,** 23–29
40. Dun, W., Jang, M, and Tseng, G. N. (1999) *Pflugers Arch.* **439,** 141–149
41. Zhao, F., Ghezzo-Schoneich, E., Aced, G. I., Hong, J., Milby, T., and Schoneich, C. (1997) *J. Biol. Chem.* **272,** 9019–9029
42. Whalley, D. W., Wendt, D. J., and Grant, A. O. (1994) in *Cardiac Arrhythmias: Mechanisms, Diagnosis and Management* (Podrid, P. J., and Kowey, P. R., eds) pp. 109–130, Williams & Wilkins, Baltimore, MD
43. Carmeliet, E. (1999) *Physiol. Rev.* **79,** 917–1017
44. Nakaya, H., Tohse, N., and Kanno, M. (1987) *Am. J. Physiol.* **253,** H1089–H1097
45. Tsushima, R. G., and Moffat, M. P. (1990) *J. Cardiovasc. Pharmacol.* **16,** 50–58
46. Jabr, R., and Cole, W. C. (1993) *Circ. Res.* **72,** 1229–1244
47. Cerbai, E., Ambrosio, G., Porciatti, F., Chiariello, M., Giotti, A., and Mugelli, A. (1991) *Circulation* **84,** 1773–1782
48. Chevion, M., Jiang, Y., Har-El, R., Berenshtein, E., Uretzky, G., and Kitrossy, N. (1993) *Proc. Natl. Acad. Sci. U. S. A.* **90,** 1102–1106
49. Oubidar, M., Boquillon, M., Marie, C., Schreiber, L., and Bralet, J. (1994) *Free Radic. Biol. Med.* **16,** 861–867
50. Ying, W., Han, S. K., Miller, J. W., and Swanson, R. A. (1999) *J. Neurochem.* **73,** 1549–1556
51. Saganich, M. J., Machado, E., and Rudy, B. J. (2001) *J. Neurosci.* **21,** 4609–4624
52. Inglefield, J. R., Wilson, C. A., and Schwartz-Bloom, R. D. (1997) *Hippocampus* **7,** 511–523